Correlated FLIM and PLIM for cell metabolism

A. Rück*, J. Breymayer, S. Kalinina
University of Ulm, Core Facility Confocal and Multiphoton Microscopy, N24,
Albert Einstein Allee 11, 89081 Ulm, Germany

ABSTRACT

Correlated imaging of phosphorescence and fluorescence lifetime parameters of metabolic markers is a challenge for direct investigating mechanisms related to cell metabolism and oxygen tension. A large variety of clinical phenotypes is associated with mitochondrial defects accomplished with changes in cell metabolism. In many cases the hypoxic microenvironment of cancer cells shifts metabolism from oxidative phosphorylation (OXPHOS) to anaerobic or aerobic glycolysis, a process known as "Warburg" effect. Also during stem cell differentiation a switch in cell metabolism is observed. A defective mitochondrial function associated with hypoxia has been invoked in many complex disorders such as type 2 diabetes, Alzheimers disease, cardiac ischemia/reperfusion injury, tissue inflammation and cancer.

Cellular responses to oxygen tension have been studied extensively, optical imaging techniques based on time correlated single photon counting (TCSPC) to detect the underlying metabolic mechanisms are therefore of prominent interest. They offer the possibility by inspecting fluorescence decay characteristics of intrinsic coenzymes to directly image metabolic pathways. Moreover oxygen tension can be determined by considering the phosphorescence lifetime of a phosphorescent probe. The combination of both fluorescence lifetime imaging (FLIM) of coenzymes like NADH and FAD and phosphorescence lifetime (PLIM) of phosphorescent dyes could provide valuable information about correlation of metabolic pathways and oxygen tension.

Keywords: FLIM, PLIM, NADH, FAD, redox ratio, pO_2, oxygen partial pressure, cell metabolism

1. INTRODUCTION

To maintain its metabolism, every cell needs to produce energy in form of adenosine triphosphate (ATP). Glycolysis, Krebs cycle and oxidative phosphorylation (OXPHOS) enable cells to gain this energy. In glycolysis, one molecule of glucose is processed to two molecules of pyruvate. Two molecules of ATP are produced and two molecules of oxidized nicotinamide adenine dinucleotide (NAD^+) are reduced to NADH + H^+. Under anaerobic conditions, the resulting pyruvate is processed to lactate by oxidation of NADH + H^+ and therefore NAD^+ is again available for the glycolysis enzyme glyceraldehyde 3-phosphate dehydrogenase. These processes take place in the cytoplasm. Under aerobic conditions, pyruvate decarboxylation occurs in mitochondria and two molecules of pyruvate are converted to acetyl-CoA while two molecules of NAD^+ are reduced to NADH + H^+. Subsequently, two molecules of acetyl-CoA enter Krebs cycle in mitochondria and generate six molecules of NADH + H^+, two molecules of reduced flavin adenine dinucleotide ($FADH_2$) and two molecules of guanosine triphosphate (GTP). During OXPHOS, electrons from NADH + H^+ and $FADH_2$ are transferred on oxidizers via redox reactions in the inner mitochondrial membrane. In this electron transport chain, complexes I to IV, ubiquinone and cytochrome c are involved. Changes in the conformation of complexes I, III and IV enable the transport of protons from NADH + H^+ and $FADH_2$ to the intermembrane space. The ATP synthase uses energy from the proton gradient in the intermembrane space to generate ATP. In OXPHOS, NADH + H^+ is reduced to NAD^+. The main reactions in glycolysis and OXPHOS are schematically demonstrated in figure 1.

*angelika.rueck@uni-ulm.de; phone +49 731 500 33700; fax +49 731 50 33709

Multiphoton Microscopy in the Biomedical Sciences XVI, edited by Ammasi Periasamy, Peter T. C. So, Karsten König,
Proc. of SPIE Vol. 9712, 971204 · © 2016 SPIE · CCC code: 1605-7422/16/$18 · doi: 10.1117/12.2213390

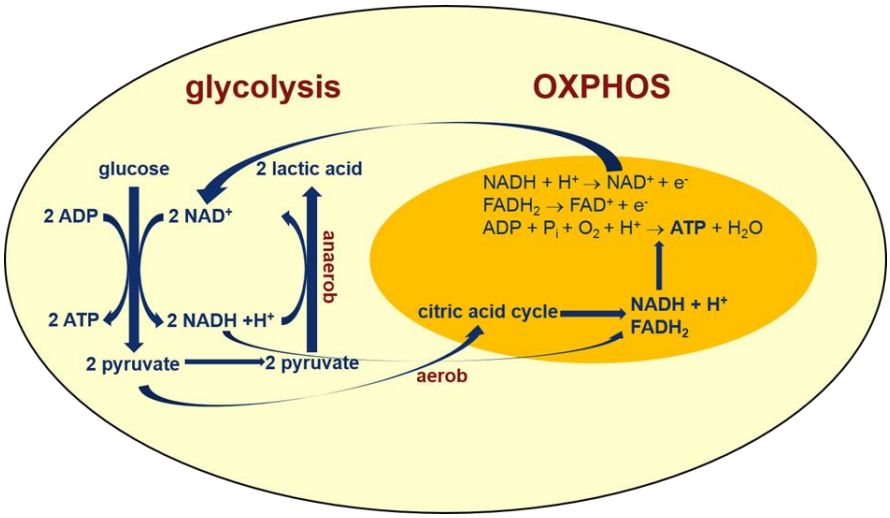

Figure 1: Main reactions involved in glycolysis and OXPHOS in a living cell to maintain energy metabolism.

Even in the presence of oxygen, cancer cells remodel their energy metabolism from OXPHOS to anaerobic glycolysis with an increased uptake of glucose, a process known as aerobic glycolysis or "Warburg effect" [1, 2]. Recent research shows that this is not true for all types of cancer cells. Whether they gain their energy from OXPHOS or glycolysis or both depends on the tumor microenvironment (hypoxia), tumor size or activated oncogenes [3, 4].

Switches in metabolism are also present in stem cells during tissue development. In pluripotent embryonic stem cells and induced pluripotent stem cells that are rapidly proliferating, metabolism corresponds to aerobic glycolysis. In differentiating embryonic stem cells, glycolysis decreases and OXPHOS increases. Quiescent adult stem cells want to avoid damage from reactive oxygen species (ROS) to ensure life-long tissue renewal capacity and reside in a hypoxic environment and therefore gain energy from glycolysis. Proliferating adult stem/progenitor cells for tissue homeostasis and renewal show a metabolism with different combinations of glycolysis and OXPHOS [5-7]. Oxygen tension therefore seems to be important as a metabolic regulator.

Identifying and characterizing the complex cellular and molecular mechanisms of energy metabolism and monitoring metabolic alterations could be useful as a biomarker for characterizing disease progression or determining the efficacy of novel therapies. Demand is high to develop robust tools for monitoring metabolic activity with high spatial and temporal resolution. Whereas spatial resolution of the widespread clinically used imaging techniques positron-emission tomography (PET) and functional magnetic resonance imaging (fMRI) is low, optical techniques based on time correlated single photon counting (TCSPC) allow high resolution on a cellular level [8]. Additionally, the development of 2-photon (2P) microscopy-based techniques profit from the spatially confined nonlinear excitation effect and deep penetrating nature of near infrared excitation light [9-12]. 2P microscopy was coupled with time-resolved fluorescence imaging microcopy (FLIM), using TCSPC methods [13, 14]. By inspecting fluorescence decay characteristics of intrinsic coenzymes 2P FLIM offer the possibility to determine redox states of cells and to directly image different metabolic pathways as glycolysis and OXPHOS which drives ATP production in the cytosol and in the mitochondria, as demonstrated in figure 1 or key ways of antioxidant defense [15, 16].

Observation of cell metabolism through time-resolved autofluorescence imaging is a new and challenging procedure (for comprehensive reviews on FLIM, see ref. [17]). It is based on the detection of the fluorescence lifetime of the metabolic coenzymes NAD(P)H (nicotinamide adenine dinucleotide (phosphate)) and FAD^+ (flavin adenine dinucleotide). These enzymes can reflect the redox state and metabolic changes during cell carcinogenesis and differentiation by the redox ratio, which is defined as the ratio of the fluorescence intensity of FAD^+ and NAD(P)H [18]. A change in the optical redox ratio causes a change in the fluorescence lifetimes of NAD(P)H and FAD^+ [19, 20]. NAD(P)H is located in the mitochondria of living cells as well as the cytoplasm. NAD(P)H not bound to proteins ("free" NAD(P)H) typically possesses a short fluorescence lifetime around 400 ps because of quenching of the reduced nicotinamide by the adenine group. If it is bound

to proteins the lifetime is much longer (1 – 6.5 ns, depending on the target to which the cofactor binds) [16, 21, 22]. Due to conformational heterogeneity of the different enzymes, bound NAD(P)H can have complex lifetime distributions with more than one exponential component [23-25]. In ref. [25] NAD(P)H fluorescence was tried to be resolved in a "quasi-global" 4-component multi-exponential fit. Also due to the existence of the two redox couples NAD+/NADH and NADP+/NADPH in the cells the lifetime of bound NAD(P)H varies [16]. The maximum emission of free NAD(P)H is around 470 nm, whereas the maximum is blue-shifted towards 440 nm when bound to proteins [26-29].

Observation of cell metabolism by autofluorescence FLIM could be a straightforward tool in fluorescence guided diagnosis. The method is even discussed to be used in the clinic for imaging of brain tumours [30, 31]. However, in contrast to most reports the lifetime of NAD(P)H was found to be longer in the tumour (glioblastoma multiforme) than in the normal tissue (normal cortex). For a comprehensive review on fluorescence lifetime techniques in medical applications see ref. [32]. A short NAD(P)H lifetime correlated with higher concentration of free NAD(P)H and glycolytic switch ("Warburg effect"), is therefore not an exclusive rule for tumors and depends on the type of cancer [15, 30, 31, 33, 34]. In a recent publication the mean lifetime of NAD(P)H of a variety of malignant breast cancer cells were increased over that of a non-cancerous mammary epithelium cell line, whereas for other types a decrease was observed [34]. Therefore, the situation is complex and more information is needed to conclude on metabolic pathways. Separation of NADH and NADPH fluorescence lifetime as described in ref. [16] is one possibility, as bound NADPH plays a role especially in antioxidant defense and could be critical to oxygen tension [35]. The involvement of both, NAD(P)H and FAD+ fluorescence lifetimes and intensities, as described for optical metabolic imaging (OMI) is important to quantify heterogeneous cell populations and to characterize the genetic and phenotypic heterogeneity of cancers [36, 37]. Substantial phenotypic variations might be induced by hypoxic stress, the mechanisms are not yet consistently known [38]. It seems that oxygen tension significantly influences metabolic pathways. Imaging methods to investigate oxygen tension are therefore of main interest.

Being a terminal electron acceptor in mitochondrial respiratory chain oxygen plays a central role in cellular energy production of mammalian organisms. Disturbance of oxygen supply induces a number of metabolic changes and can lead to cell death [39]. In fact, hypoxia associated defective mitochondrial function has been invoked in such complex disorders as type 2 diabetes, Alzheimer´s disease, cardiac ischemia/reperfusion injury, tissue inflammation and cancer [40, 41]. Therefore, measurements of oxygen level in tissue is helpful for investigation of metabolic activity under pathological conditions. Different technologies including microelectrodes, electron paramagnetic resonance (EPR) systems, nitroimidazole staining, and Raman microspectroscopy have been developed to measure oxygen in vivo and are used to monitor oxygen consumption rate and tissue oxygenation (concentration of oxygen in situ). The level of oxygen in tissue usually is evaluated as partial oxygen tension (oxygen pressure, pO2) and consequently be measured in mmHg (kPa or Torr) or in µM.

Technologies, based on phosphorescence quenching by oxygen, give rise to a generation of non-invasive optical methods for oxygen tension measurement, which permit to achieve extremely high spatial and temporal resolution. Having a triplet state as ground state oxygen is a very effective quenching agent for fluorophores in the triplet state. Generally, due to collision with an oxygen molecule the energy of phosphorescent molecules in the triplet state is transferred to oxygen instead of phosphorescence emission. Resultant decrease in intensity and lifetime of phosphorescence is described by the Stern-Volmer equation for luminescence quenching:

$$I_0/I = \tau_0/\tau = 1 + Ksv\,[Q]$$

where I and τ are luminescence intensity and lifetime in the presence of a quenching agent, I_0 and τ_0 are luminescence intensity and lifetime in the absence of a quenching agent, KSV is the Stern-Volmer constant, which quantifies the quenching efficiency and [Q] is a quencher concentration. The luminophor concentration itself is not mentioned in the equation which suggests that quenching is independent on the luminophore concentration. Oxygen tension therefore can be determined by just measuring the lifetime changes.

Lifetime measurements of oxygen sensitive probes can be performed by time resolved techniques usually by using time-gated or TCSPC methods. Application of TCSPC to confocal laser scanning microscopes provides a proper spatial resolution for detailed mapping of biological samples, loaded with pO_2-sensitive probes [42, 43, 44]. Actually, the preferred method for phosphorescence lifetime imaging (PLIM) is TCSPC in combination with confocal or multiphoton laser scanning [8, 45, 46]. Moreover, the technique of simultaneous FLIM and PLIM can be used for correlative imaging of the fluorescence lifetime of metabolic coenzymes like NAD(P)H and pO_2–sensitive phosphorescence [8, 44].

2. METHODOLOGY

2.1 Experimental Setup for simultaneous FLIM and PLIM

In order to investigate both FLIM of NADH and PLIM of pO_2-sensing $Ru(BPY)_3$, a tunable titanium-sapphire laser (Mai Tai AX HPDS, Spectra Physics) was coupled to a laser scanning microscope (LSM 710, Carl Zeiss, Germany). The Mai Tai laser is a mode-locked 80 MHz laser with a tuning range of 690 to 1040 nm, a maximum optical output power of about 2.8 W at 800 nm and a pulse width below 100 fs. Both fluorophores were simultaneously excited with two photons at 780 nm, the power at the input of the microscope was reduced and measured at the output of the objective lens to be 7.9 mW. Spectrally separated detection of NADH and $Ru(BPY)_3$ was done using a beam splitter SP 565, a band pass filter at 460/60 nm and a long pass filter LP 615 (AHF Analysentechnik, Tübingen, Germany). Two hybrid detectors were used: HPM-100-40 and HPM-100-50 (Becker & Hickl GmbH, Berlin, Germany) (see fig.2).

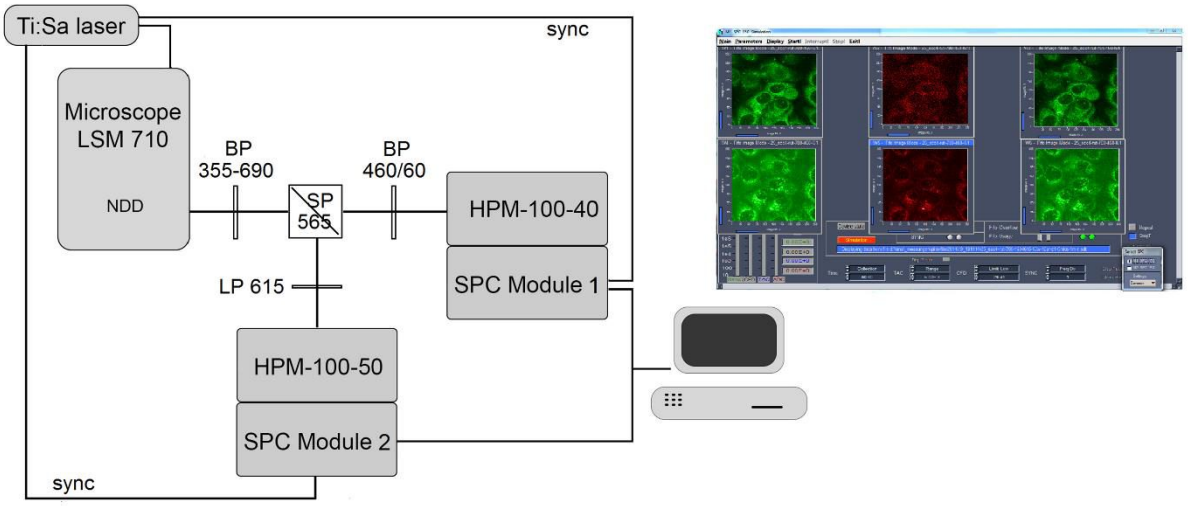

Figure 2. System for simultaneous detection of FLIM and PLIM, coupled to the NDD port of the LSM 710.

The PLIM technique is based on modulating the Ti:sapphire laser by a signal synchronously with the pixel clock of the scanner, and recording the fluorescence and phosphorescence signals by multi-dimensional TCSPC [8]. Fluorescence is recorded during the on-phase of the laser, phosphorescence during the off-phase. Laser modulation is achieved by controlling the AOM of the laser scanning microscope by a signal generated in the TCSPC system (Becker&Hickl GmbH, Berlin, Germany). This system is coupled to the NDD port of the LSM 710.

For each photon, the TCSPC module determines the location within the scanning area and the time of the photon within the laser pulse period. These parameters are used to build up a two-dimensional photon distribution over the scan area, and the time in the fluorescence decay. For the results presented below we used an image size of 256 x 256 pixels and 256 time channels. Scanning was performed at a frame time of 7.75 s, corresponding to a pixel time of 12 µs. The laser-on time at the beginning of each pixel was 2.8 µs, the time range of the PLIM recording 6.4 µs. The total acquisition time was 60 seconds. The objective lens was a EC Plan-Neofluar 40x/1,30 oil (Carl Zeiss, Jena, Germany), providing a scan area of 212.1 µm x 212.1 µm at zoom = 1.

2.2 Cell culture studies

Human oral squamous carcinoma cells (SCC-25, ATCC-Nr. CRL-1628) were grown in DMEM/F-12 (Invitrogen (Gibco), Karlsruhe, Germany) medium supplemented with 10 % fetal bovine serum (FBS) at 37° C and 5 % CO_2. For microscopy all cells were seeded on glass bottom microwell dishes with a coverglass of 0.16 to 0.19 mm (MatTek, Ashland, Massachusetts) at a density of 90 cells/mm^2 and were allowed to grow for 48 h.

Microscopic observations were performed immediately after removing the incubation medium and rinsing twice with indicator free and FBS free medium. The samples were imaged under standard conditions for cell cultivation (37 °C, 5 % CO_2).

2.3 pO_2-sensor

Ruthenium tris-(2,2'-bipyridyl) dichloride ($Ru(BPY)_3$) (Sigma-Aldrich, St. Louis, Missouri) was used as a pO_2-sensor. The stock solution was 10 mM in phosphate-buffered saline (PBS). A final concentration of 0.1 mM $Ru(BPY)_3$ was applied to cell-monolayers 16 h before FLIM-measurements.

2.4 Inhibition and scavenging of oxygen

Inhibition of mitochondrial oxidative phosphorylation was achieved with antimycin A, which was applied to the SCC-25 monolayer in 1 ml medium without supplements in a final concentration of 7.5 µM and incubated 15 minutes before the start of measurements.

Oxygen scavenger sodium sulfite (Na_2SO_3) in concentrations of 0.66 M and 2 M in DMEM/F12 without supplements was used to decrease the oxygen tension in the glass bottom dish to a level of 9.3 % and 3.2 % oxygen, respectively.

3. RESULTS

Simultaneous FLIM and PLIM of living cells was realized with the equipment presented in section 2.1. A two-photon excitation at 780 nm induced phosphorescence of $Ru(BPY)_3$ as well as fluorescence of intracellular NADH. Band-pass filter 460/60 nm selected the spectral range for NADH lifetime detection. A phosphorescent signal was not detected within this spectral range. Because of a lack of other phosphorescent molecules within the cells, it has not been necessary to use a narrow band-pass filter for imaging of $Ru(BPY)_3$. The applied long pass filter LP 615 covered the proper emission band.

$Ru(BPY)_3$ was added to the cells, which were afterwards rinsed twice to make sure that detected phosphorescence originates only from cells. FLIM and PLIM measurements were simultaneously performed and the fluorescence lifetime of NADH and the phosphorescence lifetime of $Ru(BPY)_3$ were calculated with SPCImage software from respective channels providing lifetimes for NADH within the range 650 - 1900 ps and for $Ru(BPY)_3$ within the range 200 - 600 ns. The measurement in the presence of the oxygen scavenger sodium sulfite (Na_2SO_3) in medium significantly reduced pO_2, correlated with an increased phosphorescence lifetime. In correlation to the increased phosphorescence lifetime the fluorescence lifetime of NADH significantly decreased due to oxygen scavenging.

Mitochondrial function and oxygen consumption in the cells was manipulated by blocking coenzyme Q-cytochrome c reductase (complex III) in the mitochondrial membrane with antimycin A. As demonstrated with simultaneous FLIM/PLIM this induced a significant decrease of the phosphorescence lifetime of the oxygen sensor due to increased oxygen accumulation in the mitochondrial membrane (see figure 3, right). Simultaneous FLIM/PLIM revealed that the mean fluorescence lifetime of NADH significantly decreased (see figure 3, left) which correlates to an increase of free NADH, induced by impaired oxygen reduction in the mitochondrial membrane.

4. DISCUSSION

The aim of this work was to evaluate a method for correlative NAD(P)H-FLIM and oxygen sensing-PLIM for simultaneously investigating cell metabolism and oxygen tension. Using a two channel TCSPC system with spectral separation, cell metabolism was analyzed by fluorescence lifetimes of NAD(P)H and phosphorescence lifetime of a phosphorescent oxygen probe.

The metabolic status, which can be calculated by the relation of the intracellular amount of free and protein-bound NADH can indicate a switch between glycolysis and oxidative phosphorylation. Another important parameter for the redox status of cells and tissues is the oxygen partial pressure. Besides induction of hypoxia, oxygen was modulated directly in the mitochondrial membrane. Blocking of complex III in the respiratory chain and accumulation of oxygen could be observed by both the decrease of the phosphorescence lifetime of $Ru(BPY)_3$ and a reduction of the lifetime of NADH in cell cultures. The decrease of the lifetime of NADH is a clear indication of acute changes in the redox state of the cells.

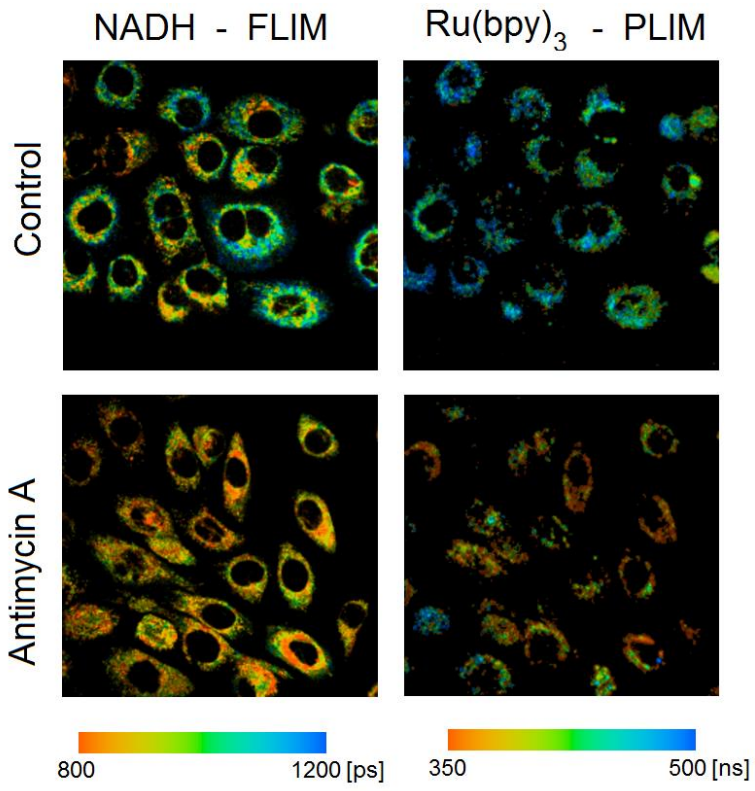

Figure 3. Simultaneous FLIM and PLIM images of control SCC-25 cells and the cells treated with antimycin A.

REFERENCES

[1] R. A. Gatenby and R. J. Gillies, "Why do cancers have high aerobic glycolysis?," Nature Reviews **4** (11), 891-899 (2004).

[2] O. Warburg, ""On the origin of cancer cells", Science **123** (3191), 309–314 (1956).

[3] C. Jose, N. Bellance, R. Rossignol, "Choosing between glycolysis and oxidative phosphorylation: A tumor's dilemma?", Biochim. Biophys. Acta **1807**(6), 552-561 (2011)

[4] J. M. Garcia-Heredia, A. Carnero, "Decoding Warburg's hypothesis: tumor-related mutations in the mitochondrial respiratory chain", Oncotarget., doi: 10.18632 (2015)

[5] N. Shyh-Chang, G.Q. Daley, L.C. Cantley, "Stem cell metabolism in tissue development and aging", Development. **140**(12), 2535-2547 (2013)

[6] M. P. De Miguel, Y. Alcaina, D.S. de la Maza, P. Lopez-Iglesias, Curr. Mol. Med. **15**(4), 343-359 (2015).

[7] A. Mohyeldin, T. Garzon-Muvdi, A. Quinones-Hinojosa, Cell Stem Cell **7**(2), 150-161 (2010).

[8] W. Becker, "Advanced Time-Correlated Single Photon Counting Applications", Springer Series in Chemical Physics, Volume 111 (Springer-Verlag Berlin Heidelberg, 2015).

[9] W. R. Zipfel, R. M. Williams, R. Christie, A. Y. Nikitin, B. T. Hyman, W. W. Webb, Live tissue intrinsic emissionn microscopy using multiphoton-excited fluorescence and second harmonic generation", Proc. Natl. Acad. Sci. U.S.A. **100**(12), 7075 – 7080 (2003).

[10] K. Svoboda, R. Yasuda, "Principles of two-photon excitation microscopy and its applications to neuroscience," Neuron **50**(6), 823 – 839 (2006).

[11] S. Huang, A. A. Heikal, W. W. Webb, "Two-photon fluorescence spectroscopy and microscopy of NAD(P)H and flavoprotein," Biophys. J. **82**(5), 2811-2825 (2002).

[12] K. Schenke-Layland, I. Riemann, U. A. Stock, K. König, "Imaging of cardiovascular structures using near-infrared femtosecond multiphoton laser scanning microscopy," Journal of Biomedical Optics. **10**(2), 240171-240175 (2005).

[13] A. Ehlers, I. Riemann, M. Stark, K. König, "Multiphoton fluorescence lifetime imaging of human hair," Microscopy Research and Technique. 7**0**(2), 154-161 (2007).

[14] W. Becker, "Advanced Time-correlated Single Photon Counting Techniques" (Springer, Berlin, 2005).

[15] A. Rück, C. Hauser, S. Mosch, and S. Kalinina, "Spectrally resolved fluorescence lifetime imaging to investigate cell metabolism in malignant and nonmalignant oral mucosa cells", J. Biomed Opt **19**(9), 096005 (2014).

[16] T. S. Blacker, Z. F. Mann, J. E. Gale, M. Ziegler, A. J. Bain, G. Szabadkai, M. R. Duchen, "Separating NADH and NADPH fluorescence in live cells and tissues using FLIM", Nature Communications **5**, 3936 (2014).

[17] A. Periasamy, R. M. Clegg, "FLIM Microscopy in Biology and Medicine" (CRC Press, New York, 2009).

[18] B. Chance, B. Schoener, R. Oshino, F. Itshak, Y. Nakase, "Oxidation-reduction ratio studies of mitochondria in freeze-trapped samples. NADH and flavoprotein fluorescence signals", J. Biol. Chem. **254** (11), 4764-4771 (1979).

[19] M. C. Skala, K. M. Riching, A. Gendron-Fitzpatrick, J. Eickhoff, K. W. Eliceiri, J. G. White, N. Ramanujam, "*In vivo* multiphoton microscopy of NADH and FAD redox states, fluorescence lifetimes, and cellular morphology in precancerous epithelia", PNAS **104**(49), 19494-19499 (2007).

[20] M. C. Skala, N. Ramanujam, "Multiphoton Redox Ratio Imaging for Metabolic Monitoring in vivo", Methods Mol. Biol. **594**, 155-162 (2010).

[21] J. R. Lakowicz, H. Szmacinski, K. Nowaczyk, M. L. Johnson, "Fluorescence lifetime imaging of free and protein-bound NADH", PNAS **89**(4), 1271–1275 (1992).

[22] Y. Wu, W. Zheng, J. Y. Qu, „Sensing cell metabolism by time-resolved autofluorescence", Opt. Lett. **31**(21), 3122-4 (2006).

[23] C. Stringari, A. Cinquin, O. Cinquin, M. A. Digman, P. J. Donovan, E. Gratton, "Phasor approach to fluorescence lifetime microscopy distinguishes different metabolic states of germ cells in a live tissue", PNAS **108**(33), 13582-13587 (2011).

[24] A. Chorvatova, A. Mateasik, D. Jr. Chorvat, "Spectral decomposition of NAD(P)H fluorescence components recorded by multi-wavelength fluorescence lifetime spectroscopy in living cardiac cells", Laser Phy. Lett **10**(12), 125703 (2013).

[25] M. A. Yaseen, S. Sakadzic, W. Wu, W. Becker, K. A. Kasischke, D. A. Boas, "In vivo imaging of cerebral energy metabolism with two-photon fluorescence lifetime microscopy of NADH", Biomed. Opt. Expr. **4**(2), 307-321 (2013).

[26] K. König, H. Schneckenburger, "Laser-induced autofluorescence for medical diagnosis", J. Fluoresc **4**(1), 17-40 (1994).

[27] J. R. Lakowicz, "Principles of Fluorescence Spectroscopy," 2nd edition Kluwer/ Academic Plenum Publishers, New York (1999).

[28] R. Huber, M. Buchner, H. Li, M. Schlieter, A. D. Sperfeld, M. W. Riepe, "Protein binding of NADH on chemical preconditioning," J. Neurochem. **75**(1), 329–335 (2000).

[29] N. L. Vekshin, "Photonics of Biopolymers" (Springer, Berlin, 2002).

[30] Y. Sun, N. Hatami, M. Yee, J. Phipps, D. S. Elson, F. Gorin, R. J. Schrot, L. Marcu, "Fluorescence lifetime imaging microscopy for brain tumor image-guided surgery", J. Biomed. Opt. **15**(5), 056022 (2010).

[31] J. Leppert, J. Krajewski, S.R. Kantelhardt, S. Schlaffer, N. Petkus, E. Reusche, G. Hüttmann, A. Giese, "Multiphoton excitation of autofluorescence for microscopy of glioma tissue", Neurosurgery **58**(4), 759-767 (2006).

[32] L. Marcu, "Fluorescence lifetime techniques in medical applications", Ann. Biomed. Eng. **40**(2), 304-331 (2012).

[33] J. McGinty, N. P. Galletly, C. Dunsby, I. Munro, D.S. Elson, J. Requejo-Isidro, P. Cohen, R. Ahmad, A. Forsyth, A. V. Thillainayagam, M. A. Neil, P. M. French, G. W. Stamp, "Wide-field fluorescence lifetime imaging of cancer", Biomed. Opt. Express **1**(2), 627-640 (2010).

[34] A. J. Walsh, R. S. Cook, H. C. Manning, D. J. Hicks, A. Lafontant, C. L. Arteaga, M. C. Skala, "Optical metabolic imaging identifies glycolytic levels, subtypes, and early-treatment response in breast cancer", Cancer Res. **73**(20), 6164-74 (2013).

[35] A. Chorvatova, S. Aneba, A. Mateasik, D. Chorvat, B. Comte, "Time-resolved fluorescence spectroscopy investigation of the effect of 4-hydroxynonenal on endogenous NAD(P)H in living cardiac myocytes", J. Biomed. Opt. **18**(6), 067009 (2013).

[36] A. J. Walsh, M. C. Skala, "Optical metabolic imaging quantifies heterogeneous cell populations", Biom. Opt. Express **6**(2), 559-573 (2015).

[37] A. J. Walsh, R. S. Cook, M. E. Sanders, L. Aurisicchio, G. Ciliberto, C. L. Arteaga, M. C. Skala, "Quantitative optical imaging of primary tumor organoid metabolism predicts drug response in breast cancer", Cancer Res. **74**(18), OF1-OF11 (2014).

[38] G. Solaini, A. Baracca, G. Lenaz, G. Sgarbi, "Hypoxia and mitochondrial oxidative metabolism", Biochim. Biophys. Acta **1797**(6-7), 1171-1177 (2010).

[39] M. C. Brahimi-Horn, J. Pouyssegur, "Oxygen, a source of life and stress", FEBS Lett. **581**(19), 3582-91 (2007).

[40] A. Mayevsky, "Mitochondrial function *in vivo* evaluated by NADH fluorescence", (Springer Cham Heidelberg New-York Dordrecht London, 2015).

[41] G. Solaini, A. Baracca, G. Lenaz, G. Sgarbi, "Hypoxia and mitochondrial oxidative metabolism", Biochim. Biophys. Acta **1797**(6-7), 1171-1177 (2010).

[42] H. Kurokawa, H. Ito, M. Inoue, K. Tabata, Y. Sato, K. Yamagata, S. Kizaka-Kondoh, T. Kadonosono, S. Yano, M. Inoue & T. Kamachi, "High resolution imaging of intracellular oxygen concentration by phosphorescence lifetime," Scientific Reports **5**, 1-13 (2015).

[43] N. A. Hosny, D. A. Lee, M. M. Knight, "Single photon counting fluorescence lifetime detection of pericellular oxygen concentrations ", J. Biomed. Opt. 17(1), 016007-1-12 (2012)

[44] S. Kalinina, D. Bisinger, J. Breymayer, A. Rück, "Cell metabolism, FLIM and PLIM and applications", Proc. SPIE **9329**, Multiphoton Microscopy in the Biomedical Sciences XV, 93290C, 2079166 (2015).

[45] R. I. Dmitriev, S. M. Borisov, A. V. Kondrashina, J. M. P. Pakan, U. Anilkumar, J. H. M. Prehn, A. V. Zhdanov, K. W. McDermott, I. Klimant, D. B. Papkovsky, "Imaging oxygen in neural cell and tissue models by means of anionic cell-permeable phosphorescent nanoparticles", Cell. Mol. Life Sci. **72**(2), 367-381 (2015).

[46] W. Becker, B. Su, A. Bergmann, K. Weisshart, O. Holub,"Simultaneous fluorescence and phosphorescence lifetime imaging", Proc. SPIE **7903**, Multiphoton Microscopy in the Biomedical Sciences XI, 790320 (2011).

ACKNOWLEDGEMENTS

This work was carried out with financial support by the Ministry of Financial Affairs of Germany, FKZ order: KF2122510AK2 ("PLIMOX") and FKZ order: IGF 18239 N ("MITOSKOPIE") and the Ministry of Research and Development, FKZ order: 13N12942 ("METAPHOR"). Sviatlana Kalinina is founded from the project MITOSKOPIE. Jasmin Breymayer is partly founded from the project METAPHOR.